HHS Public Access

Author manuscript

Cell Rep. Author manuscript; available in PMC 2017 October 23.

Published in final edited form as:

Cell Rep. 2017 May 09; 19(6): 1141–1150. doi:10.1016/j.celrep.2017.04.044.

Distinct translaminar glutamatergic circuits to GABAergic interneurons in the neonatal auditory cortex

Rongkang Deng[1], **Joseph P. Y. Kao**[2], and **Patrick O. Kanold**[1,†]

[1]Department of Biology University of Maryland, College Park, MD 20742, USA

[2]Center for Biomedical Engineering and Technology, and Department of Physiology, University of Maryland School of Medicine, Baltimore, MD 21201, USA

Summary

GABAergic activity is important in neocortical development and plasticity. Since the maturation of GABAergic interneurons is regulated by neural activity, the source of excitatory inputs to GABAergic interneurons plays a key role in development. We show by laser-scanning photostimulation that layer 4 and layer 5 GABAergic interneurons in auditory cortex in neonatal mice (< P7) receive extensive translaminar glutamatergic input via NMDAR-only synapses. Extensive translaminar AMPAR-mediated input developed during the second postnatal week while NMDAR-only presynaptic connections decreased. GABAergic interneurons showed two spatial patterns of translaminar connection: inputs originating predominantly from supragranular or from supragranular and infragranular layers including subplate which relays early thalamocortical activity. Sensory deprivation altered the development of translaminar inputs. Thus, distinct translaminar circuits to GABAergic interneurons exist throughout development and the maturation of excitatory synapses is input specific. Glutamatergic signaling from subplate and intracortical sources likely plays a role in the maturation of GABAergic interneurons.

Graphical abstract

†Corresponding Author: Lead contact: Patrick O. Kanold, Dept. of Biology, University of Maryland, 1116 Biosciences Res. Bldg., College Park, MD 20742 USA, Phone: +1 (301) 405.5741, pkanold@umd.edu.

Author contributions

RKD and POK designed research. RKD performed research and analyzed data. POK supervised research and analyzed data. POK and RKD discussed the results and wrote the manuscript. JPYK contributed reagents and edited the manuscript.

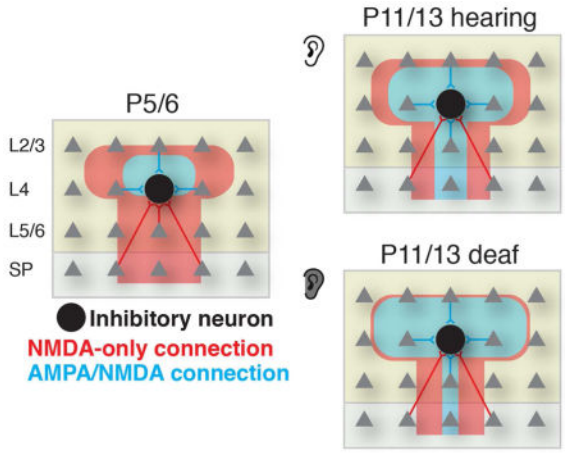

Keywords

GABA; interneuron; NMDA; silent synapse; development; translaminar; auditory cortex; subplate

Introduction

γ-Aminobutyric acid (GABA)ergic interneurons constitute 20% of cortical neurons and are crucial in shaping neural activity (Kepecs and Fishell, 2014; McBain and Fisahn, 2001). Cortical GABAergic interneurons are important for development and play diverse roles in neuronal migration, synapse formation, synchrony of network activity, and controlling the timing of the critical period (Hensch, 2005; Le Magueresse and Monyer, 2013); therefore the control of GABAergic maturation is an essential developmental process. Neural activity, especially sensory activity mediated by the thalamus, is required for the normal morphological development of interneurons from the caudal ganglionic eminence (CGE) (De Marco Garcia et al., 2011; De Marco GarcÌa et al., 2015). In particular, glutamatergic signaling via *N*-methyl-D-aspartate receptors (NMDAR) is required for interneuron maturation (De Marco GarcÌa et al., 2015). A key feature of glutamatergic transmission in the immature cortex is the presence of “silent synapses” that only contain NMDAR but not α-amino-3-hydroxy-5-methyl-4-isoxazolepropionic acid receptors (AMPAR) (Hanse et al., 2013; Isaac, 2003; Malenka and Nicoll, 1997). Silent (NMDAR-only) synapses can be converted to AMPAR-containing synapses through activity-dependent mechanisms; therefore NMDAR-only synaptic connections can precede mature neural connections (Anastasiades and Butt, 2012; Meng et al., 2014). While hippocampal interneurons have silent synapses at young ages (Matta et al., 2013; Riebe et al., 2009) the presence of silent synapses on cortical interneurons as well as the presynaptic laminar source of such synapses is unknown. Thalamic activity can reach cortical interneurons via multiple potential intra-cortical pathways such as subplate neurons, which relay thalamic input to L4 before the maturation of thalamocortical connections (Barkat et al., 2011; Kanold and Luhmann, 2010; Viswanathan et al., 2016; Zhao et al., 2009). We thus investigated the intra-cortical sources of excitatory input to developing cortical GABAergic interneurons and delineated which spatial circuits were NMDAR-only and thus might precede later mature connections.

We show by laser-scanning photostimulation (LSPS) and whole-cell patch clamp recordings in the auditory cortex that layer 4 (L4) and layer 5 (L5) GABAergic interneurons receive extensive translaminar glutamatergic input mediated by NMDAR-only synapses in neonatal mice (< P7). AMPAR-mediated input was initially low and increased rapidly during the second postnatal week. Presynaptic cells were located within the cortical plate and the thalamorecipient cortical subplate, indicating that GABAergic interneurons integrate activity across cortical laminae. GABAergic interneurons from L4 and L5 formed subclasses, integrating inputs either from supragranular and the home layer or across supragranular and infragranular layers (including subplate).

Early sensory deprivation resulted in a differential reorganization of the translaminar connectivity to GABAergic interneurons from both superficial and deep layers. Since early sensory information is relayed via the subplate indirectly and directly to GABAergic interneurons, our findings suggest that glutamatergic signaling from subplate and intracortical sources via NMDARs play a role in mediating the excitation and maturation of GABAergic interneurons, and that early sensory experience can shape this process.

Results

To visualize GABAergic interneurons in brain slices, we crossed the *Gad2* Cre mouse line (JAX 010802) with the floxed-tdTomato Ai9 mouse line (JAX 007909) to express red fluorescent protein (RFP) in GABAergic interneurons. The *Gad2* promoter is active in a large number of cortical GABAergic interneurons with some bias towards CGE-derived GABAergic interneurons (López-Bendito et al., 2004; Taniguchi et al., 2011). We used the *Gad2* Cre mouse line since other driver lines, e.g. Parv-Cre, do not express at sufficient levels at young ages. Guided by RFP expression, we performed whole-cell patch clamp recordings from 109 GABAergic interneurons in L4 and L5 in thalamocortical slices of the auditory cortex (Figure 1A).

Post-recording staining and reconstruction showed that patched *Gad2* interneurons had various morphology (Figure S1A), suggesting that this transgenic line targets a diverse population of GABAergic interneurons. In particular, in the older age group, multiple distinct morphological classes based on dendritic arbors were present, which is consistent with adult morphology (Ascoli et al., 2008; DeFelipe et al., 2013). Dendritic arbors could span across multiple laminae and could reach the pia at the youngest ages (Figure S1A), and gross quantification of the morphological features showed that the number of nodes, the number of ends and total neurite length tended to increase during the first 2 weeks of development (Figure S1B). Notably, these parameters showed large variability in the oldest group, possibly reflecting morphological heterogeneity. Together these results show that even at the youngest ages, *Gad2* interneurons extend their dendrites into multiple cortical layers.

Gad2 interneurons receive translaminar AMPAR inputs that increase over development

The presence of extensive dendritic arbors at the youngest ages suggested that GABAergic interneurons may already receive extensive synaptic inputs from different layers. Indeed, cortical GABAergic interneurons express functional glutamatergic receptors early during

development (Bartolini et al., 2013; Le Magueresse and Monyer, 2013) and thus likely receive inputs from cortical and subcortical excitatory neurons. In adult thalamocortical inputs target both excitatory and inhibitory neurons in L4 (Ji et al., 2016). Since thalamocortical inputs to L4 in auditory cortex (ACX) are not mature until about P12 (Barkat et al., 2011), we speculated that ACX GABAergic interneurons at neonatal ages receive most excitatory input from excitatory cortical neurons. To identify glutamatergic input to GABAergic interneurons, we used whole-cell patch clamp to record from identified GABAergic interneurons (Figure 1B) combined with LSPS with caged-glutamate to focally stimulate cortical neurons. To isolate AMPAR-mediated excitatory postsynaptic currents (EPSCs) we performed experiments in voltage clamp (V_{hold} = −70 mV); $GABA_A$ currents were blocked with picrotoxin. We typically stimulated at least 480 locations spanning all cortical layers around the recorded neuron (Figure 1A and S1C) (Meng et al., 2014; Viswanathan et al., 2012). Laser power and recording conditions were similar to our prior study at the same ages, which ensured reliable stimulation of excitatory neurons while minimizing polysynaptic transmission (Meng et al., 2014). In particular, prior cell-attached recordings have shown that our stimulus paradigm reliably activates neurons in all layers during the studied age range (Meng et al., 2014). When the focused laser spot was close to the recorded cell, glutamate receptors on the recorded cell could be directly activated (Figure 1C). These direct activations of the recorded neuron were distinguished from synaptic EPSCs by their short latency and verified by their resistance to TTX whereas synaptic responses had longer latency and were sensitive to TTX (Figures 1C and 1D).

We next investigated whether the spatial pattern of AMPAR-mediated input to L4 GABAergic interneurons changed over early neonatal development. In particular, between P5 and P13 thalamocortical circuits in A1 undergo significant developmental changes as thalamic input, which is initially relayed to L4 by subplate neurons, directly activates L4 by P12 (Barkat et al., 2011; Zhao et al., 2009). We thus compared GABAergic interneurons from before to after ear opening (P11/12). For each cell, we plotted the locations where EPSCs could be evoked (“input map”). As shown in the exemplar neuron (Figures 1E and S1C), excitatory inputs originated from locations near the soma. We quantified both the peak amplitude and charge of the evoked EPSC (Figure 1E) (Meng et al., 2014). To reveal the general features of the input patterns, we aligned the cell somata of the population and averaged the input maps from multiple cells recorded for each age group to derive a spatial map of connection probability (Figure 2A; average soma location indicated with white circle). To visualize the diversity of laminar input we also plotted the laminar input for every cell in our population (Figure 2B). *Gad2*-positive L4 GABAergic interneurons received local synaptic input from surrounding cortical excitatory neurons as early as P5 (Figures 2A–2C). In addition, some neurons (4/26 = 15%) received input from the subplate (SP) (Figures 2B, D, E). In the second postnatal week, in particular after ear opening, additional inputs were present especially from deeper cortical layers such as L5/6 but also from L2/3 (Figures 2A and 2B). At later ages inputs from all layers increased, but the relative increase was largest for inputs originating in L5/6 (Figures 2D and 2E). Overall, the laminar balance of inputs to L4 *Gad2* interneurons shifted from being dominated by L4 and L2/3 inputs to receiving over 30% of inputs from deep sources. Thus, L4 *Gad2* interneurons at all ages integrate information over multiple layers.

To characterize if increased inputs also lead to increased spatial integration, for each cell we calculated the distance in the rostro-caudal (tonotopic) direction that contained 80% of all AMPA mediated connections (Figure 2F). We find that with age inputs arose from more distant locations.

To determine if the observed developmental changes are specific for L4 GABAergic interneurons or if they represent a general developmental progression of GABAergic interneurons, we repeated these experiments in L5 GABAergic interneurons. Similar to their L4 counterparts, L5 GABAergic interneurons received synaptic input from surrounding cortical excitatory neurons as early as P5 (Figure S2A–C). The amount of input also increased in the second postnatal week, especially after ear opening (Figure S2C–D). In contrast to L4 interneurons however, L5 *Gad2* interneurons showed significantly increased input from L2/3, L4, and subplate but not L5/6 (Figures S2D, 3E). Over development the proportional input from each layer showed only slight relative decreases in L5/6 input, and matching slight relative increases in L2/3 input over development (Figure S2E). Like L4 GABAergic interneurons, spatial integration also increased for L5 GABAergic interneurons in development (Figure S2F).

Functional glutamatergic signaling between neurons also depends on the synaptic strength of the EPSCs between cells. We thus measured the strength of the connection by calculating the charge of the evoked EPSC at each stimulation site. Over development the average EPSC charge and peak amplitude increased in L4 but not L5 *Gad2* interneurons (Figure S3B and D), suggesting increased strength of synaptic connections. Together these results show that initially GABAergic interneurons in L4 and L5 receive mostly sparse AMPAR-mediated inputs, but that later they receive extensive excitatory translaminar inputs and thus integrate information from all cortical laminae.

GABAergic interneurons at the earliest ages receive extensive translaminar inputs mediated by NMDARs only

Our anatomical reconstructions show that even at the youngest ages, *Gad2* interneurons extend their dendrites into multiple cortical layers but the LSPS results show that these neurons received only few inputs outside their home layer. AMPAR-mediated synaptic transmission is not the only form of glutamatergic transmission. The immature cortex contains NMDAR-only synapses (Hanse et al., 2013; Isaac, 2003; Malenka and Nicoll, 1997). To investigate the existence of NMDAR-only inputs to GABAergic interneurons, we held each cell at −70 mV as well as at +40 mV (Figure 3A). Since $GABA_A$ currents were blocked with picrotoxin, the only synaptic currents present at +40 mV were glutamatergic currents carried by AMPA and/or NMDA receptors. NMDAR-only input was identified when a single pair of stimuli at a given location evoked a synaptic response only at the +40 mV holding potential but not at −70mV (Figures 3B, S1C, D). Neurons that showed only local AMPAR-mediated inputs (Figure 3C, same cell as Figure 1F) could show extensive NMDAR-only inputs and NMDAR-only inputs were sensitive to AP5 (Fig. S1D–F). We thus investigated the spatial pattern of NMDAR-only inputs to *Gad2* L4 and L5 interneurons during development. At the youngest neonatal ages the connection probability maps showed extensive NMDAR-only inputs from stimulation sites surrounding L4 *Gad2* interneurons

during the neonatal stage as well as a large fraction of inputs from stimulation sites within L5/6 and subplate (18/26 = 69% neurons have subplate inputs) (Figure 4A, B). A similar pattern of additional translaminar inputs from L5/6 and subplate was seen in L5 *Gad2* interneurons (Figure S2G–H). The NMDAR-only inputs diminished during the second postnatal week (Figures 4A). For L4 *Gad2* interneurons there was a small decrease in the amount of NMDAR-only inputs (Figures 4C), especially from L2/3 and L4 (Figure 4D). Accordingly, the proportion of inputs from supragranular layers decreased and the proportion of inputs from infragranular layers increased (Figure 4E). Calculating the distance in the tonotopic direction that contained 80% of all NMDA-only inputs showed that with age inputs arose from more distant locations (Figure 4F).

L5 *Gad2* interneurons also showed NMDAR-only synapses which, in contrast to AMPAR-mediated inputs that originated mostly in L4 and L2/3, originated in L5/6 and subplate (Figure S2G–L). There was a small decrease in the amount of NMDAR-only inputs from L4 and L5/6 (Figure S2J). Importantly, in both L4 and L5 GABAergic interneurons a large number of NMDAR-only inputs remained at the oldest ages studied and those inputs predominantly originated in L5/6 and subplate (Figures 4D, E and S2J–K). However, the low spatial probability at older ages is lower probably due to increased spatial integration at older ages (Figure S2L). Thus, the NMDAR-only inputs became more spatially dispersed. The average charge and peak amplitude of connections showed a small decrease in the charge of the synaptic connections, but no significant change in the peak amplitude (Figure S3F and H).

The data above suggest a developmental change in excitatory inputs for *Gad2* interneurons. Input from cortical excitatory neurons was primarily mediated by NMDAR-only synapses during neonatal stage (P5/6), the AMPAR-mediated inputs increased rapidly during the second postnatal week. To demonstrate this change, we calculated the ratio of NMDAR-only inputs to AMPAR-mediated inputs. The median ratio was around 3 in the neonatal group, indicating a dominant contribution of NMDAR-only inputs at the neonatal stage (Figure S4). Over development, with the increase of AMPAR-mediated inputs, the ratio gradually decreased.

Together our results show that L4 and L5 *Gad2* GABAergic interneurons receive extensive glutamatergic inputs from intracortical sources in multiple layers and that at early ages these inputs are mediated by NMDA receptors. L4 and L5 interneurons differ in the origins of their NMDAR-only inputs: L4 interneurons tend to receive more supragranular inputs while L5 interneurons receive more infragranular inputs. Both populations of cells also receive inputs from the subplate. Thus, GABAergic interneurons integrate activity from multiple cortical layers from the earliest stages of cortical development.

The maturation of glutamatergic input to MGE-derived *Lhx6* interneurons follows a similar developmental trajectory to *Gad2* interneurons

Our studies so far relied on the *Gad2* transgenic mouse. Since the *Gad2* promoter is biased towards CGE-derived GABAergic interneurons (López-Bendito et al., 2004; Taniguchi et al., 2011), we tested if our observed developmental trajectory also applied to other populations of GABAergic interneurons, e.g., those derived from the medial ganglionic eminence

(MGE). Thus, we repeated our study using *Lhx6*-GFP mice, which primarily labels MGE-derived GABAergic interneurons (Cobos et al., 2006; Du et al., 2008; Fogarty et al., 2007; Liodis et al., 2007). L4 *Lhx6* interneurons showed a similar developmental increase of AMPAR-mediated inputs as well as existence of early NMDAR-only inputs as *Gad2* L4 cells (compare Figure S5 and Figures 2 and 4). Thus, while subtle differences might exist between the various classes of GABAergic interneurons, the commonalities suggest that the developmental trajectory we uncovered is a core principle of the development of all GABAergic interneurons.

GABAergic cells show distinct translaminar input patterns

Our data so far show that GABAergic interneurons integrate excitatory input from many cortical layers. However, there was substantial variation in the amount of inputs neurons received from each layer, which suggests that different neurons may integrate across different layers, which would be consistent with the diverse morphologies observed in GABAergic interneurons (Ascoli et al., 2008; DeFelipe et al., 2013) (Figure S1A). To identify differences in translaminar integration, we quantified the columnar depth of AMPAR-mediated inputs for each cell (Figures 5A, S6–7). Cells seemed to fall into two groups, with some cells received mostly local inputs while others showed extensive translaminar integration, especially from deep layers. K-means clustering on the columnar depth of AMPAR, NMDAR-only or joint profiles (Figure S6) to identify cell groups with different ability to integrate translaminar inputs showed that L4 *Gad2* interneurons separated into two groups with a split at ~500 μm integration distance (Figure 5A, S6). While one group of L4 interneurons (group β) showed mostly local inputs (< 500 μm), another group (group α) showed greater ability to integrate translaminar inputs with a large fraction extending into the subplate (>800 μm) (Figures 5A, S6–7). Group α *Gad2* interneurons received more total AMPAR-mediated inputs and they tended to receive more AMPAR-inputs from infragranular layers (Figure 5B). However, around half of group β *Gad2* interneurons received NMDA-R only inputs from deep layers (Fig. S6). L5 *Gad2* interneurons did not clearly separate into clusters based on columnar extent, indicating that L5 *Gad2* interneurons might be more uniform than L4 *Gad2* interneurons (Figures S6–7). However, forcibly separating L5 *Gad2* interneurons into two groups by using K-means clustering resulted in similar spatial differences in input patterns as in L4 neurons (Figures S6–7), indicating that the lack of separation could be due to smaller population size (34 L5 vs. 59 L4 neurons).

The percentage of neurons in the more distal AMPAR input receiving group α tended to increase during development (L4 *Gad2* interneurons: P5/6: 11.5%; P8/9: 36.3%; P11–P13: 100%. L5 *Gad2* interneurons: P5/6: 11.1%; P8/9: 50%; P11–P13: 63.6%). The average connection probability maps of group α also showed the difference in the laminar connectivity (Figures 5C and S7C). While no L4 interneurons fell into the second group after P11, 4 of 11 L5 cells received only local inputs. This indicates that while all L4 *Gad2* interneurons receive AMPAR translaminar input in older animals, parallel circuits are present in L5. In contrast, in young animals in which group β *Gad2* interneurons dominate, around half of these interneurons receive distal NMDAR-only inputs. These data suggest that over development cortical GABAergic interneurons in each layer form at least 2

functional translaminar circuits. One predominantly receives inputs from developing supragranular layers, and another that predominantly receives inputs from infragranular layers including the subplate.

Translaminar circuits to GABAergic interneurons are altered after sensory deprivation

Neural activity reshapes cortical circuits and is required for the normal development of CGE-derived, Re-positive and Cr-positive GABAergic interneurons (De Marco Garcia et al., 2011; De Marco GarcÌa et al., 2015). Since GABAergic interneurons receive inputs from thalamorecipient layers such as the subplate and L4 at the earliest ages, the translaminar excitatory circuits onto GABAergic interneurons might be altered by sensory experience. To block auditory stimuli in our young *Gad2* transgenic animals we deafened animals by cochlear removal at P6. We then recorded L4 *Gad2* interneurons at age P13–14 and tested if deafening resulted in altered excitatory circuits to GABAergic interneurons (Figure 6). Qualitatively, the average connection maps for AMPAR mediated connections suggested increased inputs from L2/3 after deafening (Figure 6A–C, S8A). However, the amount of inputs from each lamina was unchanged, likely due to high variability between cells (Figures 6D, E). We next tested if sensory experience alters the spatial pattern of inputs from each lamina. For each cell we calculated the distance in the rostro-caudal (tonotopic) direction that contained 80% of all AMPAR mediated inputs (Figure 6F). In cells from deaf mice we find that overall inputs seemed to arise from more distant locations in L2/3 while inputs from L5/6 originated from a narrower area (Figure 6F). Thus, while sensory experience is not required for the upregulation of AMPARs in L4 GABAergic interneurons, sensory deprivation alters the spatial pattern of AMPAR-mediated excitatory connections to L4 GABAergic interneurons. Moreover, sensory deprivation differentially alters AMPA-R mediated connections from supragranular and infragranular layers in that neurons from deafened animals integrate supragranular inputs from a larger distance while infragranular inputs originate from a more spatially restricted area. Sensory deprivation also affected the numbers and spatial distribution of NMDAR-only connections. Connections mediated by NMDAR-only synapses was increased from L2/3 (Figures 7A–E, S8C, D). Spatial analysis revealed that inputs from within L4 originated from a larger distance and that inputs from SP originated closer to the soma (Figure 7F). Thus, sensory experience alters the amount and spatial patterns of NMDAR-only synapses. Together with the AMPAR results this indicates that sensory deprivation results in an increase of inputs from a larger area in supragranular layers while inputs from infragranular layers including subplate are reduced and originate from a narrower area. Our findings suggest that sensory experience is required for the refinement of excitatory connections to interneurons, but that excitatory connections can develop in the absence of sensory experience.

Discussion

We reveal early translaminar glutamatergic circuits to developing L4 and L5 GABAergic interneurons in ACX. During neonatal ages, these circuits are primarily mediated by NMDAR-only connections. During the 2nd postnatal week AMPAR-mediated connections develop. Thus, intra-cortical glutamatergic inputs contribute to the activity of GABAergic interneurons through NMDAR-only connections at neonatal ages and AMPAR-connections

at older ages. Our study here reveals the spatial pattern of the functional excitatory circuits associated with inhibitory neurons in L4 and L5 and shows that GABAergic interneurons play an important translaminar integrative function from the earliest ages on. Moreover, we show that the same neuron can receive inputs from presynaptic neurons via NMDAR-only and from other presynaptic neurons via AMPAR-containing connections. Thus, the maturation of excitatory connections on GABAergic interneurons is input-specific.

We find that cochlear ablation at P6 altered the spatial pattern of AMPAR-meditated connections assayed at P13–P14. While ear opening in C57/Bl6 mice is around P11, loud stimuli or self-generated noise can potentially drive sensory activity to regulate the refinement of glutamatergic inputs to GABAergic interneurons.

During development, silent synapse number decreases due to insertion of AMPARs (Hanse et al., 2013; Isaac, 2003; Malenka and Nicoll, 1997). While we find increased AMPAR-inputs, there is only a small decrease in NMDAR-only input number to GABAergic interneurons from P5/P6 to P11–P13. Since the number of synaptic sites increases with dendritic growth during the 2nd postnatal week, this increase might compensate for the loss of NMDAR-only connections due to synaptic maturation. Indeed, the ratio of NMDAR-only to AMPAR mediated connections decreased during the 2nd postnatal week, suggesting decreased functional contribution of NMDAR-only connections. Glutamate spillover from synaptic sites can potentially activate extrasynaptic receptors (Kullmann and Asztely, 1998; Thomas et al., 2011). Thus, even though we activate only few action potentials in presynaptic neurons, which reduces the chance for such spillover, some of the NMDAR-only connections we reveal here could potentially be the result of spillover at the level of individual synapses.

Sensory activity mediated by excitatory NMDA inputs to GABAergic interneurons plays an important role in GABAergic maturation (De Marco GarcÌa et al., 2015). Our results show that sensory evoked activity from the thalamus can reach GABAergic interneurons via multiple pathways, either via direct NMDAR-only connection from subplate or indirectly via subplate connections to cortical excitatory L4 neurons and the early NMDAR-only intra-cortical connections.

L5b Somatostatin (SST) interneurons of the earlier developing somatosensory cortex receive thalamic input and form a transient circuit to L4 during development (starting at P4) (Marques-Smith et al., 2016; Tuncdemir et al., 2016). Since our sample might include SST-neurons, translaminar excitatory circuits might couple thalamorecipient subplate and L5 SST-neurons at early ages, and both pathways converge onto L4 (Marques-Smith et al., 2016; Zhao et al., 2009). Thus, ascending input from the thalamus can reach L4 via multiple pathways.

Many (~70%) GABAergic interneurons receive subplate input. Subplate neurons are important because they are the first cortical neurons to receive thalamic inputs and because they relay these inputs into the developing cortical plate before thalamocortical inputs mature (Kanold and Luhmann, 2010; Viswanathan et al., 2016; Zhao et al., 2009). Subplate neurons are required for the maturation of thalamocortical connections (Kanold et al., 2003),

cortical network activity (Dupont et al., 2006; Kanold et al., 2003; Kanold and Luhmann, 2010; Tolner et al., 2012), and for the maturation of inhibitory transmission (Kanold and Shatz, 2006). Our results suggest that the maturational role of subplate neurons on inhibition (Kanold and Shatz, 2006) might be mediated by direct and indirect subplate inputs to GABAergic interneurons.

Based on the extent of translaminar integration GABAergic interneurons form multiple classes. Neuronal activity in superficial layers is dominated by cortically generated spontaneous activity (Khazipov and Luhmann, 2006), whereas subplate neurons relay early sensorily-evoked and peripherally-generated spontaneous activity (Kanold and Luhmann, 2010). Thus, GABAergic interneurons may differentially relay peripherally- and centrally-generated activity, consistent with deafening differentially affecting superficial and deep inputs. Since deafening altered the spatial pattern but did not prevent the development of AMPAR-meditated connections, intra-cortical activity might be sufficient for the development of AMPAR-mediated connections.

In summary, GABAergic interneurons receive extensive translaminar excitatory inputs throughout development and most inputs are mediated by NMDAR-only synapses at early ages and AMPAR-containing synapses at older ages. Although sensory experience alters the spatial pattern of superficial and deep layer inputs, excitatory inputs from other layers develop normally. Thus, the maturation of glutamatergic inputs to GABAergic interneurons is input specific and both extrinsic and intrinsic factors, such as sensory experience and cortical spontaneous activity, play a role.

Experimental Procedures

All procedures were approved by the University of Maryland Institutional Animal Care and Use Committee.

Animals

Gad2 Cre mice (JAX 010802, Jackson Laboratories) (Taniguchi et al., 2011) were bred with Ai9 transgenic mice (JAX 007909, Jackson Laboratories) to generate *Gad2* Cre tdTomato pups. Breeding pairs of *Lhx6*-GFP mice were generously provided by Dr. Gord Fishell (New York University). Mouse pups of both sexes from postnatal day 5 (P5) to P15 were used to make thalamocortical slices (Zhao et al., 2009). Slices were incubated in artificial cerebrospinal fluid (ACSF) containing (in mM): 130 NaCl, 3 KCl, 1.25 $NaHCO_3$, 10 glucose, 1.3 $MgSO_4$ and 2.5 $CaCl_2$ (pH 7.35–7.4). The ACSF was equilibrated with 95% O_2-5% CO_2.

Electrophysiology

Fluorescence targeted recordings were performed (Meng et al., 2014) with 4–9 MΩ borosilicate recording electrodes filled with internal solution containing (in mM): 115 cesium methanesulfonate, 5 NaF, 10 EGTA, 15 CsCl, 3.5 MgATP and 3 QX-314 (pH 7.25; 300mOsm). Biocytin (0.5%) was added to the internal solution. Recordings were done at room temperature and high divalent ACSF was used to reduce polysynaptic transmission. High-divalent ACSF contain (in mM): 124 NaCl, 5 KCl, 1.23 NaH_2PO_4, 26 $NaHCO_3$, 10

glucose, 4 $MgCl_2$ and 4 $CaCl_2$. Picrotoxin (100 μM) was used to block $GABA_A$ receptor mediated currents. Data were acquired with a voltage-clamp amplifier (Multiclamp 700B; Molecular Devices) and digitized using a DAQ board (NI PCI-6259, National Instruments) using EPHUS (Suter et al., 2010) in MATLAB (The Mathworks). 10 mV of estimated liquid junction potential was used to correct membrane voltages. Series resistance was typically between 20 – 40 MΩ.

Laser-scanning photostimulation

LSPS was performed as described previously (Meng et al., 2014). 0.8 mM Caged glutamate [*N*-(6-nitro-7-coumarylmethyl)-L-glutamate] (Kao, 2006; Muralidharan et al., 2016) was added to the high divalent ACSF during recording. Laser stimulation (1 ms) was delivered through a 10x water immersion objective (Olympus). Laser power on specimen was < 25 mW. For each map, an array of up to 30 × 30 sites with 40 μm spacing were stimulated once at 1 Hz in a pseudorandom order. This stimulation paradigm evokes action potential at the stimulation sites with similar spatial resolution (about 100 μm) over cells in all cortical layers during development (Meng et al., 2014; Viswanathan et al., 2012; Zhao et al., 2009). Putative monosynaptic currents (EPSCs) in GABAergic interneurons were classified by the post-stimulation latency of the evoked current. Evoked currents with latencies of less than 10 ms are likely to be the results of direct activation of glutamate receptors on the patched cell. Evoked currents with latencies between 10 ms and 50 ms are classified as monosynaptic evoked EPSCs (Figure 1C). A minimal peak amplitude (10 pA) was used to exclude false positive responses. This criterion was verified by repeating experiments in the presence of tetrodotoxin (TTX) in the bath solution (Figures 1C, D). The first peak amplitude and the charge (the area of EPSC in the counting window) were quantified for each synaptic response. AMPAR-mediated inputs were recorded at −70 mV. Recordings done at +40 mV also included NMDAR currents. To identify NMDAR-only inputs, input maps obtained at +40 mV and −70 mV were compared for each cell. Thus, each spatial location was stimulated twice, once at +40mV and once at −70 mV. Inputs from a spatial location that were only present at a holding potential of +40 mV were identified as NMDAR-only input (Figure 3). It is possible that a given presynaptic neuron makes multiple synapses with a postsynaptic cell and that one synapse is NMDAR-only and another contains AMPARs. With our method, we cannot resolve such a scenario and would score this connection as AMPAR-mediated. Thus, on an individual synaptic level we might underestimate the numbers of NMDAR-only synapses.

LSPS reliably evoked 1–2 action potentials in presynaptic neurons when the laser is targeted to ~100 μm of the cell body (Meng et al., 2014; Viswanathan et al., 2012; Zhao et al., 2009). Thus, our stimulation paradigm spatially oversampled the cortical space 2.5x in each axis. Thus, neighboring stimulation spots activate similar presynaptic cells.

Deafening

Bilateral cochlear ablation was performed at P6 in *Gad2* RFP mice. In brief, mice were deeply anesthetized by isoflurane (1.5 – 2.5%) and the surgical site was locally anesthetized by applying lidocaine. A small incision was made under the ear. The tympanic bulla was carefully removed by fine forceps and cochlea was aspirated using a glass pipette. The

surgery-induced deafness was confirmed by the lack of auditory startle responses at P13–P15.

Data analysis and statistics

Data were analyzed by custom software written in MATLAB. Cortical layer boundaries were identified by features in the brightfield image as previously described (Meng et al., 2014; Viswanathan et al., 2012; Zhao et al., 2009). For identifying subplate, the boundary between cortex and subcortical axonal fibers was identified first in the brightfield image. Evoked events were classified as direct or monosynaptically evoked EPSC by latency as detailed above. We then calculated for each cell how many spatial locations overall and how many spatial locations in each layer gave rise to monosynaptically evoked EPSCs. We also calculated the fractional input from each layer by dividing the number of stimulus locations that yielded responses in each layer by the total number of effective stimulus locations. We derived maps of average connection probability for each age group or connection patterns by aligning cells in each group to their soma and then calculating for each spatial location the fraction of cells that received an input from that location and the average EPSC strength of all inputs from each location (Meng et al., 2014).

Partitioning of cells into groups based on connection patterns was performed in MATLAB (release 2015a) by K-means clustering (Statistics Toolbox, ver. 10) minimizing the sum of the absolute differences (the L1 distance). We quantified the laminar extent (in μm) of AMPAR and NMDAR-only connections (pia to white matter) and then clustered on both (2D) AMPAR and NMDAR-only extent or clustered separately (1D) on either extent. We used 5 replicates to avoid local minima and determined the optimal numbers of clusters by the peak of the silhouette criterion (Fig. S6A, F). We then plotted the cells within each cluster in the 2D extent (AMPAR and NMDAR-only) space to gain a graphical representation of the input distribution of the groups (Fig. S6B–D, G–I).

To quantify the changes of spatial pattern of inputs during development and after deafening, we calculated the Euclidian distance between cell soma and each synaptic input. For inputs from each layer group, the distance covering 80% of inputs was used as the indicator of input pattern. Wilcoxon rank-sum test was used to test the statistical significance of the difference. Significance was defined as $P < 0.05$ or $P < 0.001$.

Biocytin staining and morphological reconstruction

Recorded cells were stained (Zhao et al., 2009) and reconstructed in Neurolucida (MBF Bioscience).

Pharmacology

Picrotoxin (PTX; 100 μM) was used to block $GABA_A$ receptor mediated currents. TTX (1 μM) was used to block action potentials. D-AP5 (50 μM) was used to block NMDAR. All drugs and chemicals were purchased from Sigma-Aldrich unless specified otherwise.

Supplementary Material

Refer to Web version on PubMed Central for supplementary material.

Acknowledgments

We want to thank Dr. Gordon Fishell at NYU for sharing the *Lhx6*-GFP transgenic mice, Drs. Paul Watkins & Xiangying Meng for suggestions on data analysis, Dr. Catherine Carr for sharing the stereology system, Benjamin Shuster for reconstructing morphology, Travis Babola for advice on cochlear ablations and the late Yunshu Liao for support. Supported by NIH R01 DC9607 (POK) and NIH R01 GM056481 (JPYK).

References

Anastasiades PG, Butt SJ. A role for silent synapses in the development of the pathway from layer 2/3 to 5 pyramidal cells in the neocortex. J Neurosci. 2012; 32:13085–13099. [PubMed: 22993426]

Ascoli GA, Alonso-Nanclares L, Anderson SA, Barrionuevo G, Benavides-Piccione R, Burkhalter A, Buzsáki G, Cauli B, Defelipe J, Fairén A, et al. Petilla terminology: nomenclature of features of GABAergic interneurons of the cerebral cortex. Nat Rev Neurosci. 2008; 9:557–568. [PubMed: 18568015]

Barkat TR, Polley DB, Hensch TK. A critical period for auditory thalamocortical connectivity. Nat Neurosci. 2011; 14:1189–1194. [PubMed: 21804538]

Bartolini G, Ciceri G, MarÌn O. Integration of GABAergic interneurons into cortical cell assemblies: lessons from embryos and adults. Neuron. 2013; 79:849–864. [PubMed: 24012001]

Cobos I, Long JE, Thwin MT, Rubenstein JL. Cellular patterns of transcription factor expression in developing cortical interneurons. Cereb Cortex. 2006; 16(Suppl 1):i82–88. [PubMed: 16766712]

De Marco Garcia NV, Karayannis T, Fishell G. Neuronal activity is required for the development of specific cortical interneuron subtypes. Nature. 2011; 472:351–355. [PubMed: 21460837]

De Marco GarcÌa NV, Priya R, Tuncdemir SN, Fishell G, Karayannis T. Sensory inputs control the integration of neurogliaform interneurons into cortical circuits. Nat Neurosci. 2015; 18:393–401. [PubMed: 25664912]

DeFelipe J, López-Cruz PL, Benavides-Piccione R, Bielza C, Larrañaga P, Anderson S, Burkhalter A, Cauli B, Fairén A, Feldmeyer D, et al. New insights into the classification and nomenclature of cortical GABAergic interneurons. Nat Rev Neurosci. 2013; 14:202–216. [PubMed: 23385869]

Du T, Xu Q, Ocbina PJ, Anderson SA. NKX2.1 specifies cortical interneuron fate by activating Lhx6. Development. 2008; 135:1559–1567. [PubMed: 18339674]

Dupont E, Hanganu IL, Kilb W, Hirsch S, Luhmann HJ. Rapid developmental switch in the mechanisms driving early cortical columnar networks. Nature. 2006; 439:79–83. [PubMed: 16327778]

Fogarty M, Grist M, Gelman D, MarÌn O, Pachnis V, Kessaris N. Spatial genetic patterning of the embryonic neuroepithelium generates GABAergic interneuron diversity in the adult cortex. J Neurosci. 2007; 27:10935–10946. [PubMed: 17928435]

Hanse E, Seth H, Riebe I. AMPA-silent synapses in brain development and pathology. Nat Rev Neurosci. 2013; 14:839–850. [PubMed: 24201185]

Hensch TK. Critical period plasticity in local cortical circuits. Nat Rev Neurosci. 2005; 6:877–888. [PubMed: 16261181]

Isaac JT. Postsynaptic silent synapses: evidence and mechanisms. Neuropharmacology. 2003; 45:450–460. [PubMed: 12907306]

Ji XY, Zingg B, Mesik L, Xiao Z, Zhang LI, Tao HW. Thalamocortical Innervation Pattern in Mouse Auditory and Visual Cortex: Laminar and Cell-Type Specificity. Cereb Cortex. 2016; 26:2612–2625. [PubMed: 25979090]

Kanold PO, Kara P, Reid RC, Shatz CJ. Role of subplate neurons in functional maturation of visual cortical columns. Science. 2003; 301:521–525. [PubMed: 12881571]

Kanold PO, Luhmann HJ. The subplate and early cortical circuits. Annu Rev Neurosci. 2010; 33:23–48. [PubMed: 20201645]

Kanold PO, Shatz CJ. Subplate neurons regulate maturation of cortical inhibition and outcome of ocular dominance plasticity. Neuron. 2006; 51:627–638. [PubMed: 16950160]

Kao JP. Caged molecules: principles and practical considerations. Curr Protoc Neurosci. 2006; Chapter 6(Unit 6):20.

Kepecs A, Fishell G. Interneuron cell types are fit to function. Nature. 2014; 505:318–326. [PubMed: 24429630]

Khazipov R, Luhmann HJ. Early patterns of electrical activity in the developing cerebral cortex of humans and rodents. Trends Neurosci. 2006; 29:414–418. [PubMed: 16713634]

Kullmann DM, Asztely F. Extrasynaptic glutamate spillover in the hippocampus: evidence and implications. Trends Neurosci. 1998; 21:8–14. [PubMed: 9464678]

Le Magueresse C, Monyer H. GABAergic interneurons shape the functional maturation of the cortex. Neuron. 2013; 77:388–405. [PubMed: 23395369]

Liodis P, Denaxa M, Grigoriou M, Akufo-Addo C, Yanagawa Y, Pachnis V. Lhx6 activity is required for the normal migration and specification of cortical interneuron subtypes. J Neurosci. 2007; 27:3078–3089. [PubMed: 17376969]

López-Bendito G, Sturgess K, Erdélyi F, Szabó G, Molnár Z, Paulsen O. Preferential origin and layer destination of GAD65-GFP cortical interneurons. Cereb Cortex. 2004; 14:1122–1133. [PubMed: 15115742]

Malenka RC, Nicoll RA. Silent synapses speak up. Neuron. 1997; 19:473–476. [PubMed: 9331339]

Marques-Smith A, Lyngholm D, Kaufmann AK, Stacey JA, Hoerder-Suabedissen A, Becker EB, Wilson MC, Molnár Z, Butt SJ. A Transient Translaminar GABAergic Interneuron Circuit Connects Thalamocortical Recipient Layers in Neonatal Somatosensory Cortex. Neuron. 2016; 89:536–549. [PubMed: 26844833]

Matta JA, Pelkey KA, Craig MT, Chittajallu R, Jeffries BW, McBain CJ. Developmental origin dictates interneuron AMPA and NMDA receptor subunit composition and plasticity. Nat Neurosci. 2013; 16:1032–1041. [PubMed: 23852113]

McBain CJ, Fisahn A. Interneurons unbound. Nat Rev Neurosci. 2001; 2:11–23. [PubMed: 11253355]

Meng X, Kao JP, Kanold PO. Differential signaling to subplate neurons by spatially specific silent synapses in developing auditory cortex. J Neurosci. 2014; 34:8855–8864. [PubMed: 24966385]

Muralidharan S, Dirda ND, Katz EJ, Tang CM, Bandyopadhyay S, Kanold PO, Kao JP. Ncm, a Photolabile Group for Preparation of Caged Molecules: Synthesis and Biological Application. PLoS One. 2016; 11:e0163937. [PubMed: 27695074]

Riebe I, Gustafsson B, Hanse E. Silent synapses onto interneurons in the rat CA1 stratum radiatum. Eur J Neurosci. 2009; 29:1870–1882. [PubMed: 19473239]

Suter BA, O'Connor T, Iyer V, Petreanu LT, Hooks BM, Kiritani T, Svoboda K, Shepherd GM. Ephus: multipurpose data acquisition software for neuroscience experiments. Front Neural Circuits. 2010; 4:100. [PubMed: 21960959]

Taniguchi H, He M, Wu P, Kim S, Paik R, Sugino K, Kvitsiani D, Fu Y, Lu J, Lin Y, et al. A resource of Cre driver lines for genetic targeting of GABAergic neurons in cerebral cortex. Neuron. 2011; 71:995–1013. [PubMed: 21943598]

Thomas CG, Tian H, Diamond JS. The relative roles of diffusion and uptake in clearing synaptically released glutamate change during early postnatal development. J Neurosci. 2011; 31:4743–4754. [PubMed: 21430173]

Tolner EA, Sheikh A, Yukin AY, Kaila K, Kanold PO. Subplate neurons promote spindle bursts and thalamocortical patterning in the neonatal rat somatosensory cortex. J Neurosci. 2012; 32:692–702. [PubMed: 22238105]

Tuncdemir SN, Wamsley B, Stam FJ, Osakada F, Goulding M, Callaway EM, Rudy B, Fishell G. Early Somatostatin Interneuron Connectivity Mediates the Maturation of Deep Layer Cortical Circuits. Neuron. 2016; 89:521–535. [PubMed: 26844832]

Viswanathan S, Bandyopadhyay S, Kao JP, Kanold PO. Changing microcircuits in the subplate of the developing cortex. J Neurosci. 2012; 32:1589–1601. [PubMed: 22302801]

Viswanathan S, Sheikh A, Looger LL, Kanold PO. Molecularly Defined Subplate Neurons Project Both to Thalamocortical Recipient Layers and Thalamus. Cereb Cortex. 2016

Zhao C, Kao JP, Kanold PO. Functional excitatory microcircuits in neonatal cortex connect thalamus and layer 4. J Neurosci. 2009; 29:15479–15488. [PubMed: 20007472]

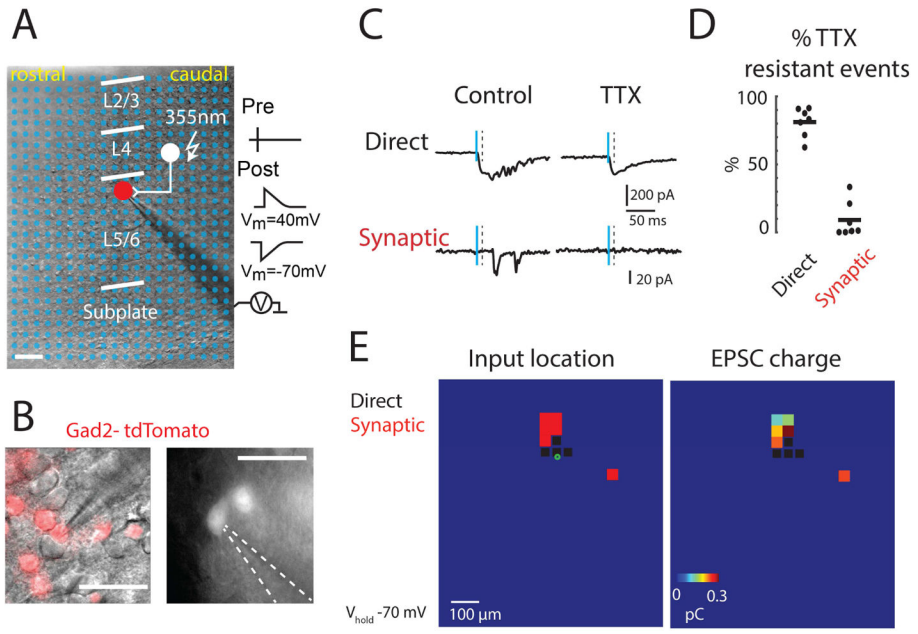

Figure 1. Laser-Scanning photostimulation (LSPS) of *Gad2* interneurons

A: An example LSPS experiment in an auditory thalamocortical slice. LSPS stimulation locations (blue dots) are superimposed on DIC image of the slice (scale bar 100 µm). Red circle indicates the soma location of the recorded interneuron. A 355-nm laser is targeted to the stimulus locations. Targeted presynaptic neuron (filled white circle) fires an action potential ('Pre' trace on the right). If the presynaptic neuron synapses on the recorded interneuron a PSC is observed ('Post' traces on the right), with the recorded neuron held at −70 mV or +40 mV for AMPAR-mediated EPSC and/or NMDAR-mediated EPSC, respectively. **B**: Images of recorded *Gad2* interneuron expressing red fluorescent protein (RFP); left frame shows RFP fluorescence superimposed on DIC image; right frame shows fluorescence from a different neuron by itself. Scale bar = 50 µm. **C:** Mapping glutamatergic inputs to GABAergic interneurons by LSPS glutamate uncaging. Traces show example responses to photostimulation at −70 mV holding potential. Vertical solid blue line indicates uncaging pulse; vertical dashed line indicates time window to discriminate direct responses. Direct activations were resistant to TTX while synaptic responses were blocked by TTX. **D:** Percentage of TTX-resistant events in the direct time window (< 10 ms latency) and synaptic time window (> 10 ms and <50 ms). 81% of short-latency (< 10 ms) responses were TTX-resistant while 8.5% of synaptic responses (> 10 ms and < 50 ms) were TTX-resistant (n = 7 cells each). **E:** Maps of an exemplar cell from P5/6 group showing stimulus locations that evoked responses and the charge at each stimulus location when V_{hold} is −70 mV. Green circle indicates soma position. Left: Map of synaptic (red) or direct (black) responses. Note that direct responses occur close to the soma. Right: Map of EPSC charge at each location. Scale bar = 100 µm.

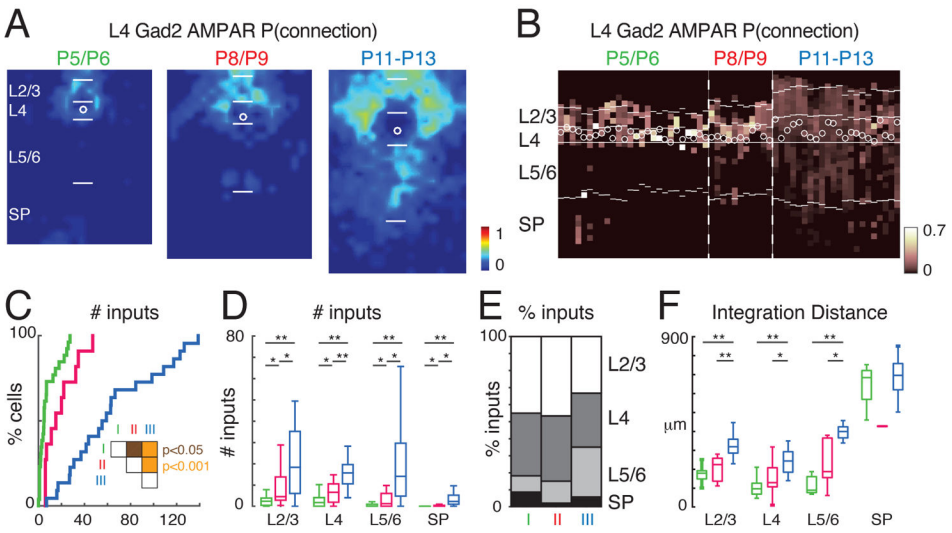

Figure 2. AMPAR-mediated cortical inputs to L4 *Gad2* interneurons increase during development

A: Map shows spatial connection probability of AMPAR-mediated inputs to layer 4 *Gad2* interneurons during development (P5/P6, n = 26 cells; P8/P9 n = 11 cells; P11–P13 n = 22 cells). The input maps (Fig. 1E) of cells were aligned to the somata and averaged. The color scale indicates the fraction of cells that received an input from a particular spatial location. AMPAR-mediated inputs increase over development. The length of bars marking the layer boundaries is 100 μm. White circles indicates soma location. **B:** Laminar distribution of inputs for each cell. Plotted is the fraction of inputs each cell received at each laminar location. Soma location is indicated by white circles; cells are aligned to L4. Layer borders for each cell are indicated by white horizontal lines. Note that a subset of cells received AMPAR-mediated input from deep layers (including subplate, SP) at P5/6. **C:** Cumulative distribution function (CDF) of the number of input locations with AMPAR responses. The amount of inputs increased during development (median ± SD P5/6: 4.86 ± 8.6; P8/9: 15.14 ± 13.96; P11–13: 57.13 ± 39.58). Significance tests between groups indicated by inset. White: $P > 0.05$, brown: $P < 0.05$, orange: $P < 0.001$. **D:** Boxplots show the amount of inputs from each layer. Inputs from all layers increased over development. Significance tests between groups indicated by horizontal bars. * $P < 0.05$, ** $P < 0.001$. **E:** Average fraction of inputs from each layer. Initially cells received most input from L2/3 and L4. **F:** Plotted is the distance that 80% of inputs from each layer originate. * $P < 0.05$, ** $P < 0.001$. Average values can be found in Supplementary Table 1.

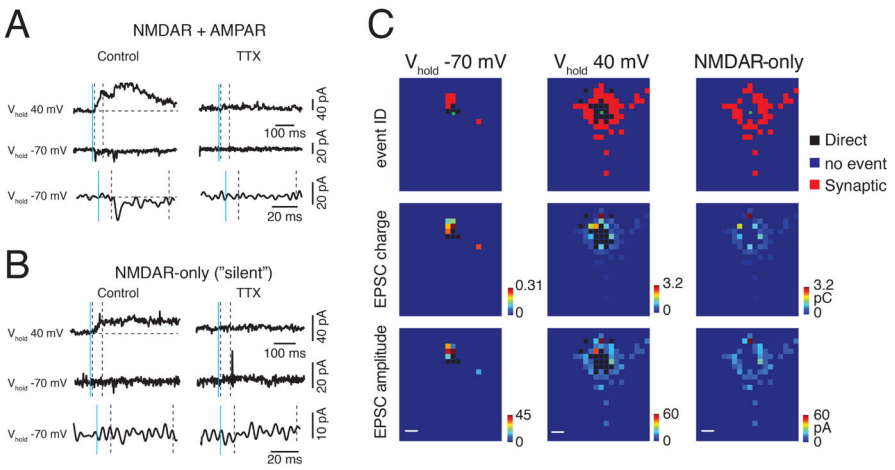

Figure 3. GABAergic interneurons have NMDAR-only synapses

A: Sample records of AMPAR-mediated synaptic inputs (lower traces with expanded scale) and NMDAR inputs (upper) revealed by LSPS glutamate uncaging experiments. EPSCs were detected at both holding potentials (−70 mV and +40 mV) for AMPAR-mediated inputs. **B**: Sample records of NMDAR-only input. EPSCs were only detectable at +40 mV holding potential. Bath application of TTX abolished the event, confirming that the responses were synaptic. Solid blue line indicates the time of uncaging; dashed black lines delimit the window for distinguishing direct activation (< 10 ms after uncaging) and synaptic inputs (> 10 ms and < 50 ms after uncaging). **C**: Representative input maps. AMPAR-mediated inputs are revealed at the holding potential of −70 mV (left); NMDAR-mediated inputs are observed at +40 mV (middle). NMDAR-only events are those where inputs are observed only in the +40 mV map (right). Pseudocolor scales for charge and peak amplitudes are shown next to each map.

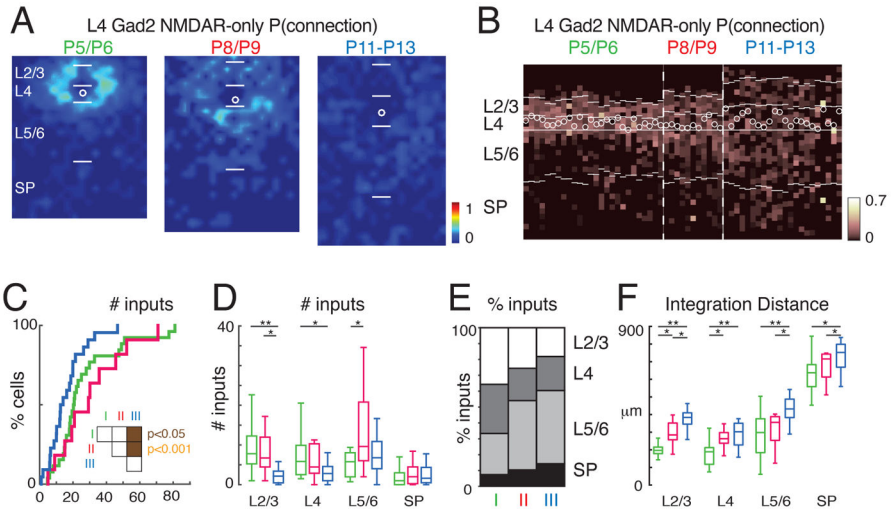

Figure 4. NMDAR-only cortical inputs to L4 *Gad2* interneurons reorganize during development

A: Average spatial connection probability maps of NMDAR-only mediated inputs to layer 4*Gad2* interneurons during development (same neurons as in Figure 2). The color scale indicates the fraction of cells that received an input from a particular spatial location. NMDAR-only input decreases over development. The length of bars marking layer boundaries is 100 μm. White circles indicates soma location. **B:** Laminar input distribution for each cell showing the fraction of input each cell received at each laminar location. Layer borders for each cell are indicated by horizontal white lines. Soma location is indicated by white circle; cells are aligned to L4. Cell order is identical to Figure 2B. Note that a subset of cells received NMDAR-only input from deep layers (including subplate) at P5/6 and that most of these cells did not receive AMPAR-mediated input from these layers. **C:** Cumulative distribution function (CDF) of the number of input locations with NMDAR-only responses. The amount of inputs decreased during development (median ± SD P5/6: 20.45 ± 19.5; P8/9: 29.23 ± 19.8; P11–13: 13.25 ± 10.8). Significance tests between groups indicated by inset. White: $P > 0.05$, brown: $P < 0.05$, orange: $P < 0.001$. **D:** Boxplots show the amount of inputs from each layer. Inputs from all layers increased over development. Significance tests between groups indicated by horizontal bars. * $P < 0.05$, ** $P < 0.001$. **E:** Average fraction of inputs from each layer. Cells received substantial input from deep layers. **F:** Plotted is the distance that 80% of inputs from each layer originate. * $P < 0.05$, ** $P < 0.001$. Average values can be found in Supplementary Table 1.

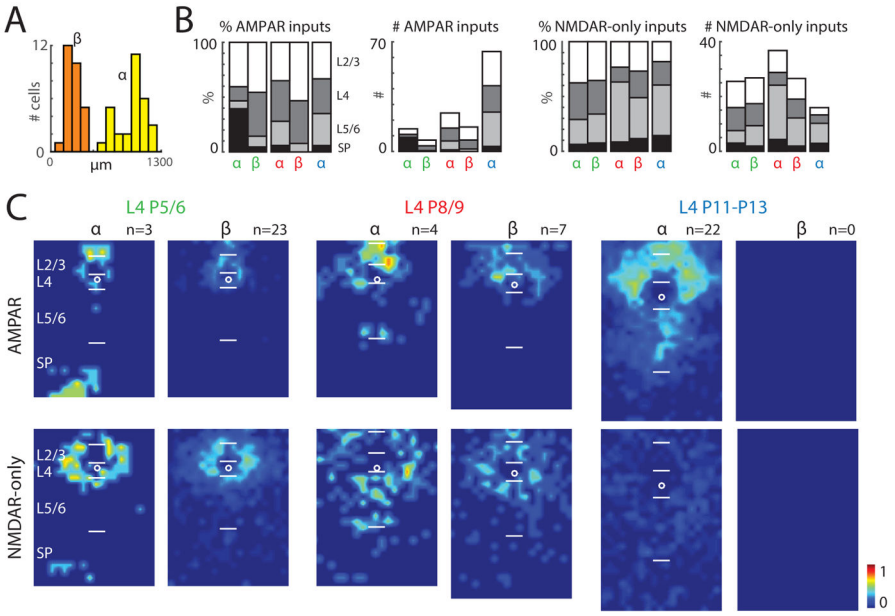

Figure 5. Two classes of GABAergic interneurons based on translaminar AMPAR-mediated inputs

A: Results of K-means clustering based on the amount of AMPAR-mediated translaminar inputs for L4 *Gad2* interneurons. Optimal cluster size of two was determined by silhouette criterion. Group α GABAergic interneurons integrate more translaminar inputs. **B:** Average fraction and average amount of inputs from each group for L4 GABAergic interneurons from different age groups. Green, P5/6; red, P8/9; blue, P11–P13. Left: AMPAR-mediated inputs, right: NMDAR-only inputs. Inputs from different layers were coded with different gray values. **C:** Average connection probability maps for L4 GABAergic interneurons in group α and β across ages. The color scale indicates the fraction of cells that received an AMPAR-mediated (top) or NMDAR-only input (bottom) from a particular spatial location. The length of bars marking the layer boundaries is 100 μm. White circles indicates soma location.

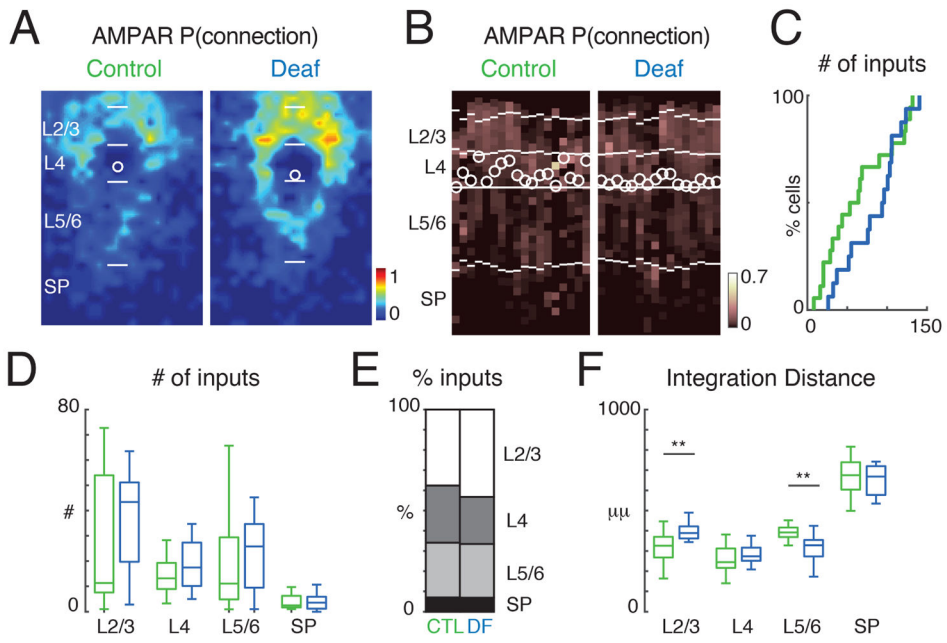

Figure 6. Sensory experience alters AMPAR connections onto GABAergic interneurons

A: Average spatial connection probability maps of AMPAR-mediated inputs to L4 *Gad2* interneurons at P13–P14 in control and deaf animals (cochlear ablation at P6) (green: control n = 18; blue: deaf n = 16). Maps show the fraction of cells that received an input from a particular spatial location. AMPAR-mediated inputs from superficial layers seem increased in deaf mice. The length of bars marking layer boundaries is 100 μm. **B:** Laminar input distribution for each cell. Plotted is the fraction of input each cell received at each laminar location. Layer borders for each cell are indicated by horizontal white lines. Soma locations are indicated by white circle; cells are aligned to L4. **C:** Cumulative distribution function (CDF) of the number of input locations. Cells from deaf mice show a trend towards increased inputs (median ± SD Control: 58.6 ± 42.6; Deaf: 94.99 ± 34.6). **D:** Boxplots show the amount of inputs from each layer. All $P > 0.05$. **E:** Average fraction of inputs from each layer. **F:** Plotted is the distance that 80% of inputs from each layer originate. Inputs from L2/3 originated further away in deaf animals ($P < 0.001$) while input from L5/6 originated from closer locations ($P < 0.001$). Average values can be found in Supplementary Table 2.

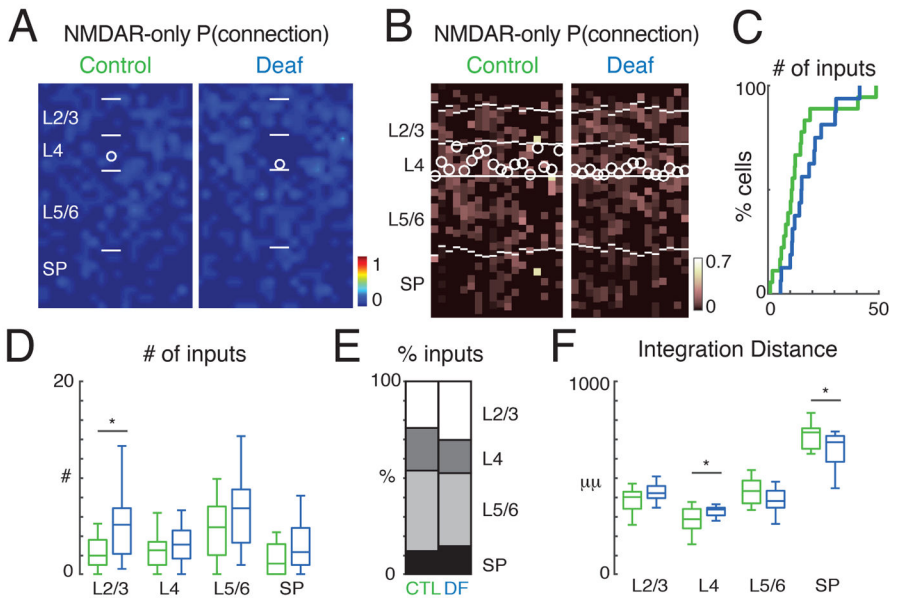

Figure 7. Sensory experience alters NMDAR-only connections onto GABAergic interneurons

A: Average spatial connection probability maps of NMDAR-mediated inputs to L4 *Gad2* interneurons at P13–P14 in control and deaf animals (same neurons as in Figure 6, green: control; blue: deaf). Maps show the fraction of cells that received an input from a particular spatial location. The length of bars marking layer boundaries is 100 μm. **B:** Laminar input distribution for each cell. Plotted is the fraction of input each cell received at each laminar location. Layer borders for each cell are indicated by horizontal white lines. Soma locations are indicated by white circle; cells are aligned to L4. **C:** Cumulative distribution function (CDF) of the number of input locations. Cells from deaf mice show a trend towards increased inputs (median ± SD Control: 10.8 ± 12.2; Deaf: 15.13 ± 9.8). **D:** Boxplots show the amount of inputs from each layer. Inputs from L2/3 are increased ($p < 0.05$), rest are all $P > 0.05$. **E:** Average fraction of inputs from each layer. **F:** Plotted is the distance that 80% of inputs from each layer originate. Inputs from L4 originated further away in deaf animals ($P < 0.05$) while input from SP originated from closer locations ($P < 0.05$). Average values can be found in Supplementary Table 2.